EasyChair Preprint

№ 10412

CFD Analysis of Different Airfoils at Various Angles of Attack

H B Shivalingaswamy, Shivprasad Panshetty, H S Shreyas, Varun Sanjay and N Vinayaka

June 16, 2023

CFD ANALYSIS OF DIFFERENT AIRFOILS AT VARIOUS ANGLES OF ATTACK

[1]Shivalingaswamy H B, [1]Shivaprasad Panshetty, [1]Shreyas H S, [1]Varun Sanjay [2] Dr. Vinayaka N
1 UG Students, Department of Aeronautical engineering, Nitte Meenakshi institute of technology Yelahanka, Bengaluru-560064
2 Associate Professor, Department of Aeronautical engineering, Nitte Meenakshi institute of technology Yelahanka, Bengaluru-560064

Abstract- *The effectiveness of the aerodynamic flow is significantly influenced by the aerodynamic airfoil blades. Selecting the correct airfoil section for the blade is essential. The angle of attack and how it impacts lift and drag forces, such as whether it creates high lift and low drag or vice versa, are crucial aspects that define the system's performance. The artwork that was exhibited was inspired by this. The study's major goal was to compare the NACA 2412, NACA 4412, NACA 23012, and NACA 23112 airfoils at various angles of attack while keeping the Reynolds number constant. The geometry and analysis were done in Ansys-Fluent, and the CFD study used the SST K-w model.* Calculations were done from a variety of attack angles. For the computational domain, an unstructured mesh with inflation and sphere of effect was selected, taking care of the grid refinement surrounding the airfoil to encapsulate the boundary layer approach. The results of the CFD simulation are very consistent with those obtained by experimentation, showing that CFD analysis is a reliable substitute for experimental methods.

Keywords: Lift Coefficient, Drag Coefficient, Angle of Attack, Airfoil

I. INTRODUCTION

An airfoil is a body's cross-section that is placed in an airstream to generate a useful aerodynamic force. Airplane wings, propeller blades, windmill blades, turbine and compressor blades, and hydrofoils are a few examples of airfoils. The amount of lift produced by an airfoil is primarily determined by its angle of attack. Although some designs can generate lift at 0 degrees AOA, most shapes require a positive angle of attack. NACA Airfoils are the aerofoil designs created by NACA (the National Advisory Committee for Aeronautics). The term "NACA" is followed by a string of numbers that characterize the form. The four- and five-digit airfoils are the most often used.
The current work intends to analyze the flow field for the NACA 2412, NACA 4412, NACA 23012, and NACA 23112airfoils at different angles of attack with constant Reynolds number of 10^6 in light of the review of the available literature. The SST k-w turbulence model was used to solve the steady-state governing equations of continuity and momentum conservation, and the findings were confirmed by comparing them to the available experimental data.

We've discussed a few fascinating recent studies on airfoils below. Patil et al. [1] investigated low Reynolds numbers in relation to lift and drag on wind turbine blades. They discovered that as the Reynolds number climbs, the lift and drag forces also rise. Haque and colleagues conducted a series of experimental studies to better understand the effects of Reynolds number and angle of attack in flow analysis. A comparison of computational and experimental data was conducted as part of Yao et al.'s [3] inquiry on the aerodynamic effectiveness of wind turbine airfoils. A comparison analysis has been done to look at how transonic flow across an airfoil affects changes in angle of attack and Mach number [4]. transonic flow over an airfoil [4]. After comparing a number of turbulence models, including Spalart-Allmaras, Realisable k, and k shear stress transfer, it was shown that these models do not yet produce correct results at high angles of attack [5]. Laminar separation bubble and laminar turbulent separation over the airfoil have been studied by Shah et al. [6] and researchers examined the relationships between the angle of attack, the Reynolds number, and the separation of the laminar bubbles. The analysis of stall angle and its effects on lift and drag coefficient was published by Sahin et al. [7]

II. AIRFOIL

An airfoil, or aero foil in British English, is a material whose velocity through a gas may produce significant lift. These include things like wings, sails, turbine blades, and propellers and rotors. Similar-functioning foils called hydrofoils use water as its operating fluid. The angle of attack of an airfoil is mostly responsible for its lift. Contrary to other foil designs that require a positive angle of attack, cambered airfoils may produce lift at zero angle of attack. Airfoils can be designed with different shapes for use at different speeds; those meant for supersonic flight are typically smaller and have sharp leading edges, whilst those meant for subsonic flight frequently have rounded leading edges. They all have a sharp trailing edge.

In some circumstances (such as inviscid potential flow), the Kutta-Joukowski theorem and the circulation principle can be utilized to directly connect the lift force to the average top/bottom velocity difference without computing the pressure. Helicopter rotor blades, fixed-wing aircraft wings, and stabilizers all use cross sections with an airfoil form. In addition, airfoils are employed in propellers, fans, compressors, and turbines. Sails are airfoils, and the centerboard, rudder, and keel of a sailboat have similar cross sections to and perform similarly to airfoils. The bodies of numerous plants and sessile invertebrates, as well as the wings of birds, the bodies of fish, and the shape of sand dollars, all contain airfoils and hydrofoils.

On a symmetric air foil, the centre of pressure and the aerodynamic centre are identical and are situated precisely one chord-length behind the leading edge.

$c_l = 2\pi\alpha$

Where c_l is the section lift coefficient,

α is the angle of attack in radians, measured relative to the chord line.

Also, as a consequence of, the section lift coefficient of a cambered airfoil of infinite wingspan is:

$c_l = c_{l0} + 2\pi\alpha$

where c_{l0} is the section lift coefficient when the angle of attack is zero.

The stall of the airfoil, which typically happens at an angle of attack between 10° and 15° for conventional airfoils, is not taken into account by the thin airfoil concept. However, Wallace J. Morris II published a theory in his PhD thesis in the middle of the late 2000s that predicted the start of leading-edge stall. The details on the current state of theoretical understanding of the leading-edge stall phenomenon are provided by Morris' further adjustments. According to Morris' hypothesis, the inner flow solution will have a global separation zone at the crucial AOA. A subsonic flow around a thin airfoil can be described in terms of two zones that asymptotically match one another: the outer area, which encloses the majority of the airfoil chord, and the inner region, which encloses the nose. Morris' equations show various features of thin airfoil theory since this theory regulates the flow in the outer region.

METHODOLOGY

MODEL CREATION

NACA 2412, NACA 23012, NACA 4412, and NACA 23112 airfoils' geometries were constructed in ANSYS WORKBENCH using their coordinates, which were imported from an online airfoil plotter. The c-shape fluid domain was utilized to generate a mesh for the computational domain's discretization. The approach of all triangles was used to generate the unstructured mesh. The intake, walls, airfoil, and outlet are all included in the mesh model. The edge sizing for the airfoil is 300 divisions, and the mesh fineness is 2. The grids are formed finely close to the airfoil portions and coarsely farther away. While NACA23012 and NACA 23112 have 77143 nodes and 150057 elements, NACA2412 and NACA 4412 have 44136 nodes and 86337 elements.

The necessary model was then created by importing the coordinates into ANSYS Fluid Flow (Fluent)-Geometry Modeler. To orient thesimulation, the current case contour is also created. The geometriesfor NACA 2412 and the other variants are shown in Fig. (1), correspondingly. The process used for the remaining three airfoils was similar.

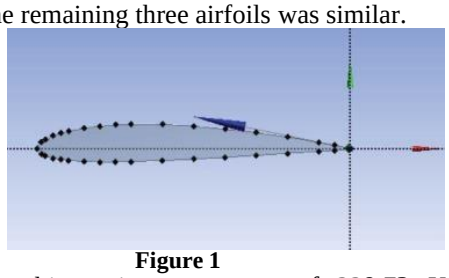

Figure 1

With an ambient air temperature of 229.73 K, an air pressure of 30.82 kPa, a freestream density of 0.4671 kg/m3, and a dynamic viscosity of 1.493 10-5 N/m-2s, the flow parameters were established for the atmospheric circumstances at a height of 9000 m.The simulation was run at Mach 0.6 under subsonic flow conditions. The resultant freestream velocity was 182.28 m/s, while the speed of sound for the flow circumstances was 303.8 m/s. The simulation's Reynolds number was 1425703.081.

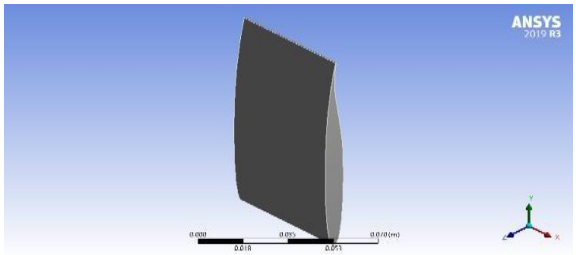

Figure 2

.

The simulation used the Shear Stress Transport k - turbulence model, a Reynolds-Averaged Navier-Stokes (RANS) model, because it can both use the k - model in the freestream region and account for the transport of the principal shear stress in adverse pressure gradient boundary layers close to the wall. A straight NACA airfoil with a 0.25 m chord length and 0.25 m span was surface-modified. The surface area of the resulting airfoil model is0.0625 m2. All modified designs were compared to the clean airfoil model.

MESHING

This procedure comprises creating a mesh that is appropriate for the geometry domain, whether it be polygonal or polyhedral. The most common applications for displaying meshing on a computer screen or for physical simulation are computational fluid dynamics (CFD) and finite element analysis (FEA).

In order to analyze fluid flow, the domains are divided into smaller subdomains, and the mesh domain accuracy increases as we go towards an airfoil design. Later, the governing equations are examined and solved inside these subdomains. The mesh profiles created for each scenario are shown in Fig. 3.C-type meshing was used to mesh each and every airfoil.

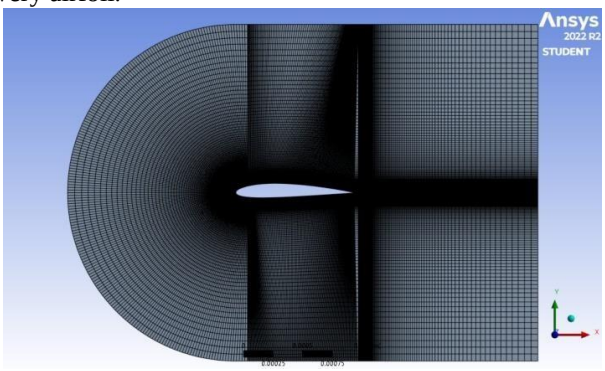

Figure 3

III. BOUNDARY CONDITION AND INPUT

Table 1 – Input and Boundary Condition

Sl No	Parameter	Value
1	Flow medium	Air
2	Flow velocity	5 & 15m/s
3	Density	1.225kg/m^3
4	Chord length	0.1m
5	Angle of attack	-15,-10,-5,0,5,10,15 degrees
6	Turbulent model	K-ω SST
7	Kinematic viscosity	1.7894e-05 kg s/m^2

Table 2 – lift, drag coefficients for NACA2412 at V=5m/s.

Sl no	Angle of attack	Coefficient of lift	Coefficient of drag
1	-15	-7.1884e-06	4.2274e-06
2	-10	-5.9854e-06	3.4159e-06
3	-5	-3.3484e-06	2.9758e-06
4	0	4.4334e-07	2.8539e-06
5	5	4.2413e-06	3.0163e-06
6	10	7.2278e-06	3.4562e-06
7	15	9.1350e-06	4.2295e-06

Table 3 – lift, drag coefficients for NACA4412 at V=5m/s.

Sl no	Angle of attack	Coefficient of lift	Coefficient of drag
1	-15	-7.3240e-02	1.3756e-01
2	-10	-2.1306e-01	1.6816e-01
3	-5	-1.4046e-01	1.6250e-02
4	0	5.2343e-03	1.8293e-04
5	5	1.1845e-02	2.3864e-04
6	10	1.7664e-02	3.5449e-04
7	15	2.0880e-02	6.8885e-04

Table 4- Coefficient of lift and drag for NACA23012 at V=5m/s.

Sl no	Angle of attack	Coefficient of lift	Coefficient of drag
1	-15	-4.4680e-01	1.7405e-01
2	-10	-5.9652e-01	1.4076e-01
3	-5	-3.8050e-01	1.5532e-02
4	0	1.1371e-01	1.3521e-02
5	5	6.1046e-01	1.6381e-02
6	10	1.0653e+00	2.4602e-02
7	15	1.2313e+00	6.1423e-02

Table 5 – Coefficient of lift and drag for NACA23112 at V=5m/s

Sl no	Angle of attack	Coefficient of lift	Coefficient of drag
1	-15	-2.0753e-01	2.0369e-01
2	-10	-3.8189e-01	3.1855e-01
3	-5	-4.3394e-01	1.7620e-02
4	0	1.0324e-01	1.5704e-02
5	5	6.1377e-01	1.8947e-02
6	10	1.0578e+00	2.8211e-02
7	15	7.9097e-01	1.0122e-01

Table 6-coefficient of lift and drag for NACA2412 for V=15m/s

Sl no	Angle of attack	Coefficient of lift	Coefficient of drag
1	-15	-4.7758e-05	2.7315e-05
2	-10	-3.6845e-05	1.9091e-05
3	-5	-2.7185e-05	1.5059e-05
4	0	3.2252e-06	1.4156e-05
5	5	3.3889e-05	1.5452e-05
6	10	5.4262e-05	1.9291e-05
7	15	7.0881e-05	2.7232e-05

Table 7– lift, drag coefficients for NACA4412 at V=15m/s

Sl no	Angle of attack	Coefficient of lift	Coefficient of drag
1	-15	-1.2926e-01	1.2076e-01
2	-10	-6.2664e-01	1.7614e-02
3	-5	-1.2084e-01	1.2081e-02
4	0	4.0423e-01	1.2060e-02
5	5	9.1341e-01	1.5976e-02
6	10	1.3552e+00	2.4186e-02
7	15	1.6046e+00	4.6148e-02

Table 8— lift, drag coefficients for NACA23012 at V=15m/s

Sl no	Angle of attack	Coefficient of lift	Coefficient of drag
1	-15	-4.5990e-01	1.7016e-01
2	-10	-9.0312e-01	2.6868e-01
3	-5	-3.8714e-01	1.3309e-02
4	0	1.1473e-01	1.1520e-02
5	5	6.2268e-01	1.4142e-02
6	10	1.0965e+00	2.1233e-02
7	15	1.4010e+00	4.1553e-02

Table 9— lift, drag coefficients for NACA23112 at V=15m/s

Sl no	Angle of attack	Coefficient of lift	Coefficient of drag
1	-15	-3.5931e+00	1.0270e+00
2	-10	-1.4707e+00	3.9096e-01
3	-5	-1.8596e+00	2.3833e+00
4	0	9.0341e-01	1.1153e-01
5	5	5.6812e+00	1.3531e-01
6	10	1.0019e+01	2.0329e-01
7	15	5.6035e+00	2.7783e+00

IV RESULTS AND DISCUSSIONS

FOR V=5m/s of NACA2412

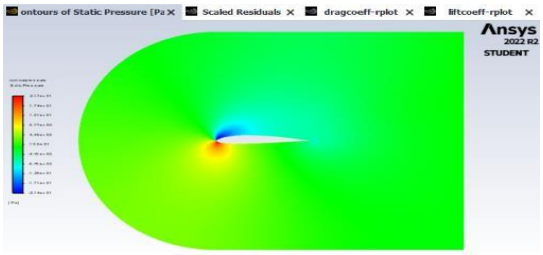

Figure 4-Pressure contour at AOA=15degree

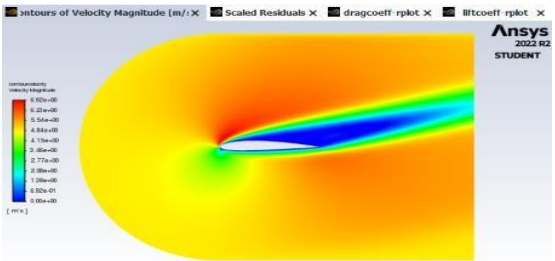

Figure 5-Velocity contour at AOA=15degree

For 15degree AOA the pressure contour is almost similar to 10degree AOA and the maximumvalue is 2.17e+01 and the maximum velocity is in velocity profile is 6.92e+00 and flowseparation starts occurring as seen

FOR V=15m/s of NACA2412

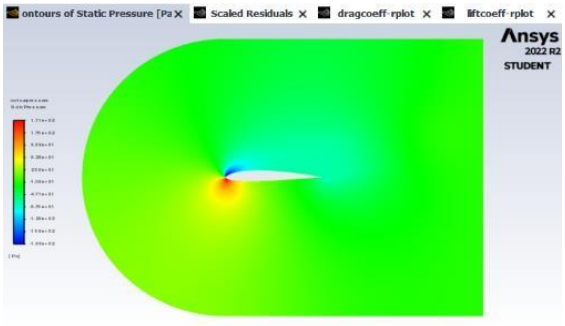

Figure 6-Velocity contour at AOA=15degree

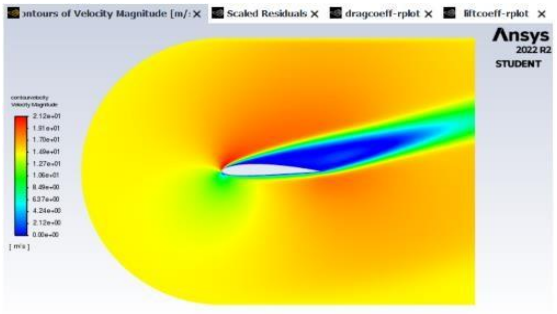

Figure 7-Velocity contour at AOA=15degree

For 15degree AOA the pressure contour is almost similar to 10degree AOA and the maximumvalue is 2.23e+01 and the maximum velocity is in velocity profile is 2.12e+01 and flow separation starts playing a major role.

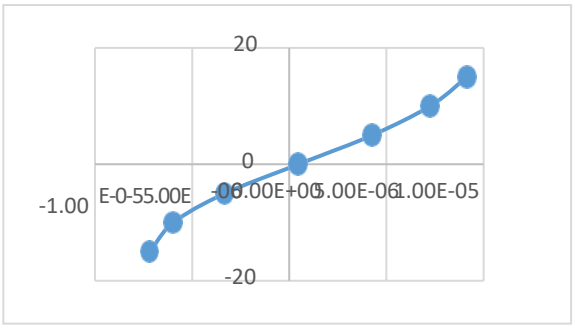

Figure 8- CL vs α at V=5m/s for NACA2412

As the AOA is changed for the NACA2412 airfoil from -15 to +15 degrees, the coefficient of lift rises. coefficient of drag falls until 0 degrees before progressively rising for positive AOA.

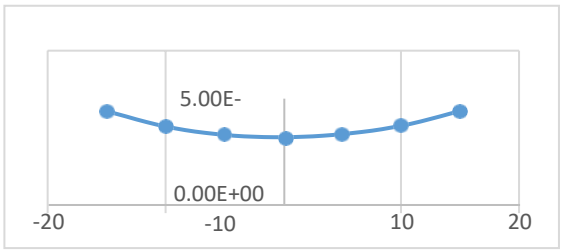

Figure 9-CD vs α at V=5m/s for NACA2412

coefficient of drag falls until 0 degrees before progressively rising for positive AOA, as seen inFig9.

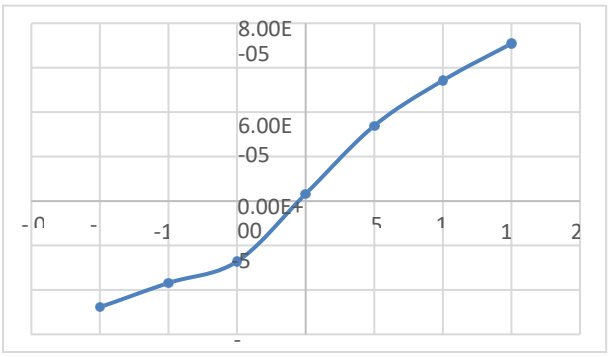

Figure 10- CL vs α at V=15m/s for NACA2412

The coefficient of lift for NACA2412 first gradually increase for negative Angle of attack and then increases suddenly as it is increased from -10degree seen in fig10

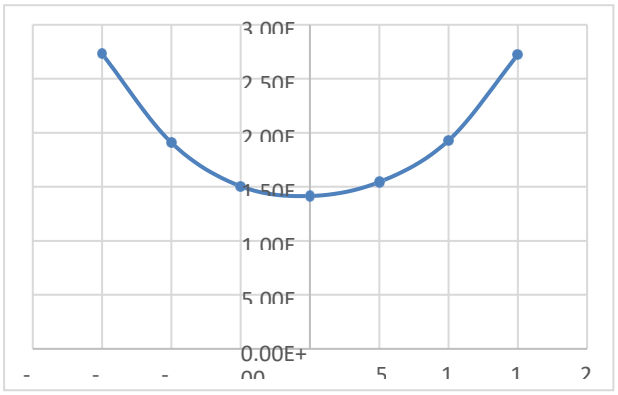

Figure 11- CD vs α at V=15m/s for NACA2412

From figure11 we can concur that the coefficient of drag decreases rapidly and then increases gradually as the angle of attack gets positive.

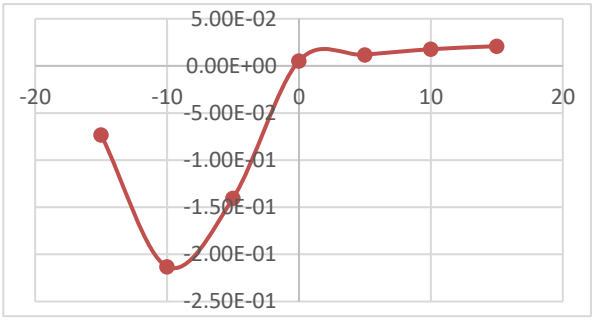

Figure 12- CL vs α at V=5m/s for NACA4412

The coefficient of lift for NACA4412 first decreases for negative Angle of attack and then increases as it is increased from -10degree seen in fig12.

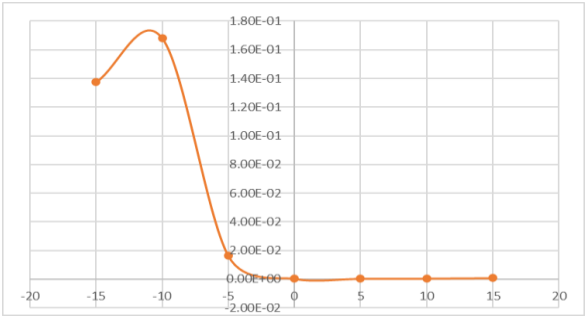

Figure 13- CD vs α at V=5m/s for NACA4412

From figure we can concur that the coefficient of drag decreases rapidly and then increases gradually as the angle of attack gets positive.

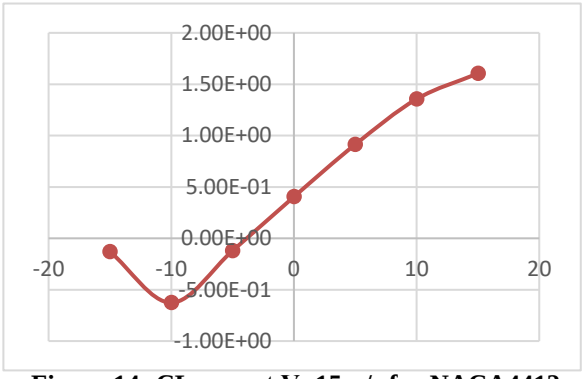

Figure 14- CL vs α at V=15m/s for NACA4412

The coefficient of lift for NACA4412 first decreases for negative Angle of attack and then increases as it is increased from -10degree seen in fig.14.

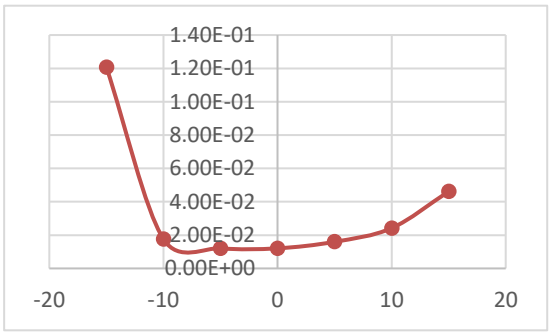

Figure 15- CD vs α at V=15m/s for NACA4412

From figure 15 we can concur that the coefficient of drag decreases rapidly and then increases gradually as the angle of attack gets positive.

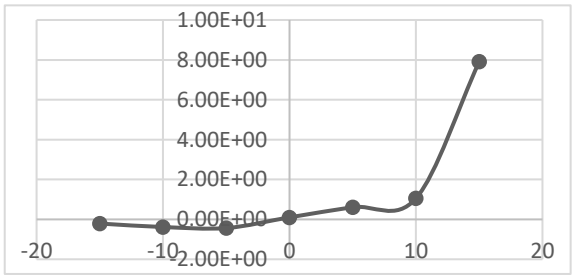

Figure 16- CL vs α at V=5m/s for NACA23112

From fig.16 As the AOA rises, the coefficient of lift for the NACA23112 airfoil drops, then increases from -5 degrees AOA.

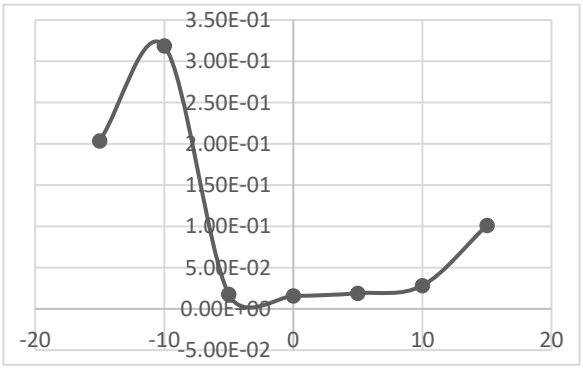

Figure 17- CD vs α at V=5m/s for NACA23112

The coefficient of drag rises until -10 degrees AOA, then decreases until 0 degrees AOA, then rises exponentially until 15 degrees AOA, as illustrated in Fig 17.

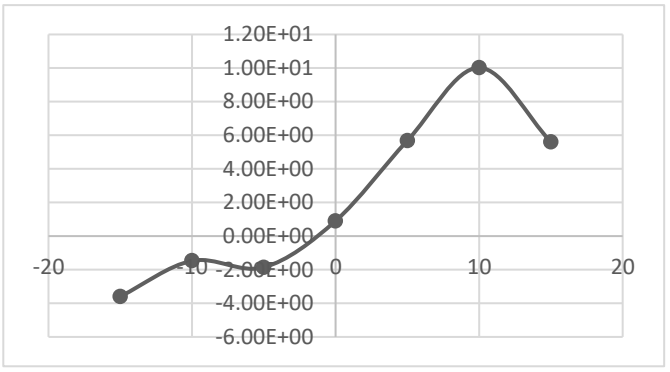

Figure 18- CL vs α at V=15m/s for NACA23112

For NACA23112 the coefficient of lift as seen in fig 18 first increases and then decreases for an angle of attack of -10 and -5degree and then increases till 10degree but then decreases for 15degree angle of attack.

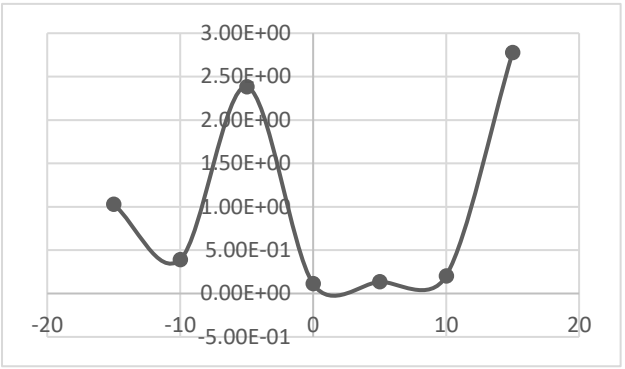

Figure 19- CD vs α at V=15m/s for NACA23112

From fig.19 The coefficient of drag is more complex to study and can be said that the drag coefficient first decreases and then increases till -5degree but then decreases as angle of attack becomes 0 but increases again for positive angle of attack.

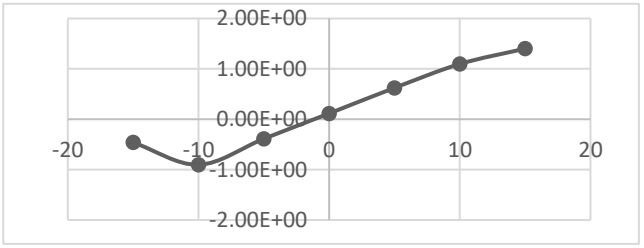

Figure 20- CL vs α at V=5m/s for NACA23012

As AOA fluctuates from -15 to -5 degrees, the coefficient of lift for the NACA23012 airfoil falls, and then it increases as AOA climbs positively, as shown in figure 20.

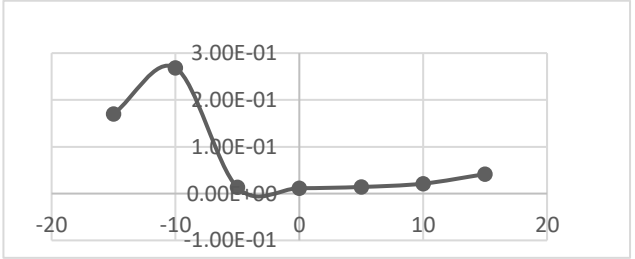

Figure 21- CD vs α at V=5m/s for NACA23012

Conversely, the coefficient of drag increases until -10 degrees, and then it lowers for positive AOA as seen in fig21.

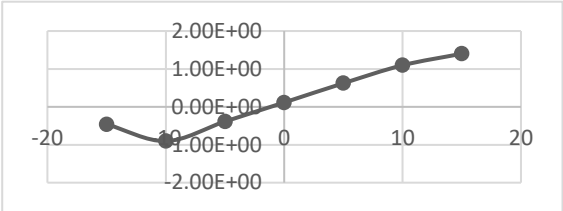

Figure 22- CL vs α at V=15m/s for NACA23012

For NACA23012, figs.22 depicts the coefficient of lift variation with angle of attack and we see that as the angle of attack increases from -15degree, CL decreases but at -5degree it starts increasing.

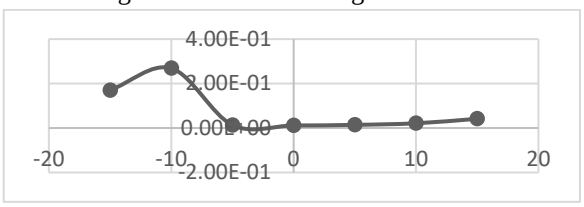

Figure 23- CD vs α at V=15m/s for NACA23012

Also, from fig.23 the variation of drag with angle of attack is such that it first increases till -10degree and then decreases till 0degree and then increases gradually for positive angle of attack.

Distribution of pressure on the airfoil

The following graphic displays the pressure distribution contours at various AOA as determined by CFD calculations. It was discovered that the airfoil's leading edge has a high-pressure area and its upper portion has a low-pressure area. Maximum pressure is seen in the airfoil's lowerarea as AOA is raised. As a result, the lift force causes the airfoil to be propelled upward towards the incoming flow stream.

Distribution of velocity on the airfoil

On the upper part of the airfoil, the flow speeds up, while on the lower part, it slows down. As AOA approaches 10 degrees and beyond, backflow generation is seen at the trailing edge,and so on.

IV.CONCLUSION

1. Ansys-Fluent was used to analyze the aerodynamic performance of NACA 2412, 4412, 23012, and 23112 at different angles of attack (-15, -10, -5, 0, 5, 10, and 15) with a Reynolds number of 1425703.081.
2. As the AOA is changed for the NACA2412 airfoil from -15 to +15 degrees, the coefficient of lift rises (figures 8 and 10) while the coefficientof drag falls until 0 degrees before progressively rising for positive AOA, (Figures 9 and 11).
3. As seen in Figs.12 and 14, the coefficient of lift for the NACA4412 airfoil reduces until -10 degrees and then increases as the AOA increases, whereas the coefficient of drag increases initially until -10 degrees and then lowers as the AOA is raised. (Figures 13 and 15).
4. As the AOA rises, the coefficient of lift for the NACA23012 airfoil drops, then increases from -5 degrees AOA, (Figures 20 and 22) whereas the coefficient of drag rises until -10 degrees AOA, then decreases until 0 degrees AOA, then rises exponentially until15 degrees AOA, as illustrated in Figures 21 and 23).
5. As AOA fluctuates from -15 to -5 degrees, the coefficient of lift for the NACA23112 airfoil falls, and then it increases as AOA climbs positively, as shown in figures 16 and 18. Conversely, the coefficient of drag increases until -10 degrees, and then it lowers for positive AOA.(Figures 17 and 19).

I. REFERENCES

[1] Ankan Dash,CFD analysis of wind turbine airfoil at various angles of attack.

[2] D.N. Srinath, Sanjay Mittal., Optimal aerodynamic design of airfoils in unsteady viscous flows, Computer Methods in Applied Mechanics and Engineering, 2010, 199, 1976 –1991.

[3] Mehmet Numan Kaya,Ali Riza Kok,Comparison of aerodynamic performances of various airfoils from different airfoil families using CFD.

[4] Lissaman. P. B. S, Low-Reynolds number airfoils, Annual Review of Fluid Mechanics. 1983, 15: 223–239.

[5] Chandrakant Sagat,Pravin Mane,Experimental and CFD analysis of airfoil at low Reynolds number.

[6] Sai Priyanka Kojja , Bijli C. Mathew, J. V. Muruga lal Jeyan,."Aerodynamics and flow separation investigation of NACA2412 and NACA23012 airfoils with dual vents at predefined separation region", AIP Publishing,2020

[7] Zubin Zahir,Gopakumar S Nair , K E Reby Roy, Vineeth Ragipathi, U V Niranjan." CFD analysis of the performance of different airfoils in ground effect.",Journal of Physics:Conference series, 2019 D.N. Srinath, Sanjay Mittal., Optimal aerodynamic design of airfoils in unsteady viscous flows, Computer Methods in Applied Mechanics and Engineering, 2010, 199, 1976 – 1991.

[8] D.J. Butter., Recent Progress on Development and Understanding of High Lift Systems, Improvement of Aerodynamic Performance Through Boundary Layer Control and High Lift Systems, Defense Technical information center, 1984, 1.1-1.26.

[9] G.Iuso, M.Onorato., Turbuluent boundary layer manipulation by outer layer devices, Mechanical 1995, 30, 359 – 76.

[10] Livya. E, G. Anitha and P. Valli., Aerodynamic analysis of dimple effect over aircraft wing, International Journal of Mechanical, Aerospace, Industrial, Mechatronic and Manufacturing Engineering, 2015, 9(2), 350-353.

[11] E Hosseini,CFD analysis of the aerodynamic characteristics of biconvex airfoil at compressible and high mach no's flow.

[12] Wong. S. F and S. S. Dol., Simulation Study of Vehicle drag reduction by surface dimples, International Journal of Mechanical and Mechatronics Engineering, 2016, 10(3), 560 -565. S.P. Venkatesan, V. Praveen Kumar, M. Sunil Kumar and Suraj Kumar

[13] Srivastav. D., Flow controls over airfoils using different shaped dimples, 2012 International Conference on Fluid Dynamics and Thermodynamics Technologies (FDTT 2012) IPCSIT vol.33(2012) 92-97. IACSIT Press, Singapore

[14] Chear. C. K and S. S. Dol, Vehicle Aerodynamics: Drag Reduction by Surface Dimples, International Journal of Mechanical, Aerospace, Industrial, Mechatronic and Manufacturing Engineering, 2015, 9 (1), 202 -205.

[15] Md. Amzad Hossain, Md. Nizam Uddin, Rubiat Mustak and Mohammad Mashud,Experimental study of aerodynamic characteristics of airfoils using different shaped dimples, The International Journal of Engineering and Science,2015,4(1),13-1.